Stable Polymer Micelles Formed by Metal Coordination

ARTICLE *in* MACROMOLECULES · AUGUST 2012

Impact Factor: 5.8 · DOI: 10.1021/ma301323z

Macromolecules

Article

pubs.acs.org/Macromolecules

Stable Polymer Micelles Formed by Metal Coordination

Junyou Wang,*[,†] Martien A. Cohen Stuart,[†] Antonius T. M. Marcelis,[‡] Mathieu Colomb-Delsuc,[§] Sijbren Otto,[§] and Jasper van der Gucht[†]

[†]Laboratory of Physical Chemistry and Colloid Science, Wageningen University, Dreijenplein 6, 6703 HB Wageningen, The Netherlands

[‡]Laboratory of Organic Chemistry, Wageningen University, Dreijenplein 8, 6703 HB Wageningen, The Netherlands

[§]Centre for Systems Chemistry, Stratingh Institute, University of Groningen, Nijenborgh 4, 9747 AG Groningen, The Netherlands

S *Supporting Information*

ABSTRACT: Metal-containing polymer micelles have attracted much attention due to their potential for medical and nanotechnological applications. In this paper, we present a method to prepare stable metal-containing polymer micelles. A diblock copolymer poly(4-vinylpyridine)-*b*-poly(ethylene oxide) ($P4VP_{48}$-*b*-PEO_{193}) with terdendate ligand groups grafted to the PVP block is synthesized. Added metal ions cross-link the ligand-carrying blocks together, while the hydrophilic block stabilizes the formed coordination complex, leading to the formation of micelles. The structure and stability of the formed micelles are investigated by light scattering and cyro-TEM. The strong coordination bonds provide high stability of the micelles: adding salt or EDTA hardly affects the formed micelles.

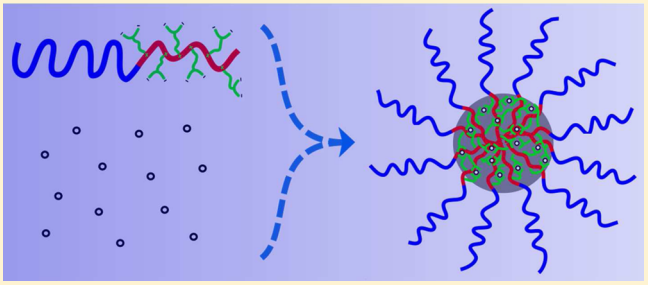

INTRODUCTION

Self-assembly based on coordination interaction is a very promising strategy for the preparation of organic−inorganic hybrid functional materials.[1−3] Metal−ligand coordination bonds have been used to build supramolecular polymers, micelles, vesicles, dendrimers, and cross-linked hydrogels.[4−6] In particular, metal-containing polymer micelles have attracted much attention because of their potential for medical or nanotechnological applications. In recent years, ingenious strategies have been developed to make such metal-containing polymer micelles. In most cases, a hydrophobic polymer is modified with a ligand group at one side of the chain. The hydrophobic parts form the micellar core, while the hydrophilic ligand groups and the coordinated metal ions are exposed to the aqueous solution.[7−9] These micelles are stabilized by the net charge of the metal−ligand complexes, which makes them rather sensitive to added salt. Schubert and co-workers have used diblock copolymers in which a hydrophilic and a hydrophobic polymer were connected by a metal coordination complex to make micelles or vesicles.[10−12] A similar strategy was followed by other groups.[13−15] More recently, Yan et al. reported a novel type of self-assembled metal-containing micelles,[16] based on the electrostatic interaction between a polycationic−neutral diblock copolymer and an anionic reversible coordination polymer consisting of metal ions coordinated by a ditopic ligand. Such metal-containing complex coacervate micelles can accommodate a large number of metal ions in the micellar core. However, the electrostatic driving force limits their stability at high ionic strength: typically, they dissociate around 200 mM salt.[17,18] In these examples, micellization is driven by either hydrophobic or ionic interactions; the metal−ligand coordination is just an assistant driving force. As an alternative strategy, the coordination interaction can also act as the direct driving force for micellization. To achieve this, a diblock copolymer consisting of a neutral hydrophilic block and a block with ligand groups is required. Added metal ions cross-link the ligand-carrying blocks together, and the formed complex is stabilized by the hydrophilic block, leading to the formation of micelles. Indeed, diblock copolymers with carboxylic groups or pyridine groups in one of the blocks were reported to form micelles with Ca^{2+} and Pt^{2+} metal ions.[19−21] However, both carboxylic and pyridine groups are monodendate ligands and only give weak coordination bonds. Here, we develop a diblock copolymer where one block carries terdendate ligand groups, which provide strong coordination bonds for micellization. The metal binding constants of the ligand groups used here are about a factor of 10^5 larger than those of pyridine or carboxylic acid groups.[22−24] The formed micelles are therefore expected to be much more stable than micelles based on either electrostatic interaction or weak coordination.

Received: June 26, 2012
Revised: August 18, 2012
Published: August 28, 2012

EXPERIMENTAL SECTION

Materials. 4-Hydroxypyridine-2,6-dicarboxylic acid (chelidamic acid) and 1,2-dibromoethane are obtained from Aldrich and used without further purification. The diblock copolymer, poly(4-vinylpyridine)-*b*-poly(ethylene oxide) (P4VP$_{48}$-*b*-PEO$_{193}$, M_w/M_n = 1.10, M_n = 13.5K) is purchased from Polymer Source. All stock solutions are prepared in MES (2-(*N*-morpholino)ethanesulfonic acid) buffer (20 mM, pH 6) with 0.1 M NaCl. The Zn-containing micelles are made by direct mixing the aqueous solutions of modified polymer and $Zn(NO_3)_2{\cdot}4H_2O$ (analytical grade).

Synthesis of the Diblock Copolymer. Synthesis of the chelidamic acid derivatives and modification of the diblock copolymer P4MVP$_{48}$-*b*-PEO$_{193}$: (a) $SOCl_2$, CH_3CH_2OH, 80 °C, reflux 20 h (67%); (b) $BrCH_2CH_2Br$, CH_3CN, 80 °C (76%).

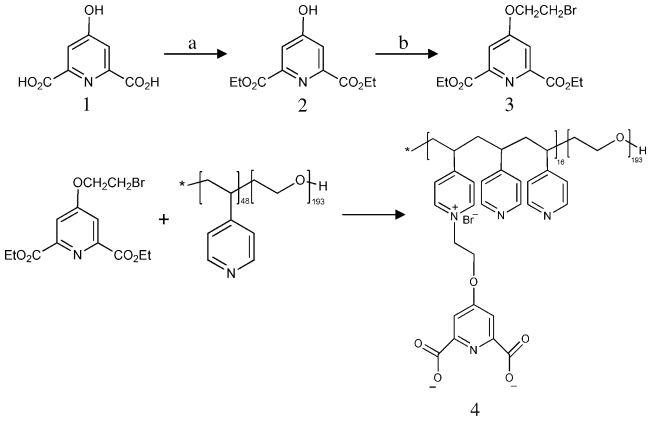

4-Hydroxypyridine-2,6-dicarboxylic acid (chelidamic acid, **1**) is esterified with ethanol to diethyl 4-hydroxypyridine-2,6-dicarboxylate (**2**).[25] Diethyl 4-(2-bromoethoxy)pyridine-2,6-dicarboxylate (**3**) is then synthesized following a published procedure.[26] The modification of the diblock copolymer P4VP$_{48}$-*b*-PEO$_{193}$ is carried out as follows: Diethyl 4-(2-bromoethoxy)pyridine-2,6-dicarboxylate (5.35 g, 15.5 mmol) and P4VP$_{48}$-*b*-PEO$_{193}$ polymer (1.0 g, 3.5 mmol pyridine groups) were dissolved in 60 mL of methanol. The solution was heated at 60 °C and refluxed for 3 days under a N_2 atmosphere. The methanol was evaporated afterward, and 5 g of K_2CO_3 and 90 mL of H_2O were then added to the residual powder, and the mixture was stirred at 70 °C for 24 h. The resulting solution was transferred to a dialysis tube and dialyzed against water for 1 week to remove all low molecular mass molecules. After the dialysis, the solution was filtrated (450 nm filter) and concentrated to a viscous phase, followed by freeze-drying from water to provide a brown product **4** (1.0 g).

The structure of the modified polymer (L-P4VP$_{48}$-*b*-PEO$_{193}$) was confirmed by ^{1}H and ^{13}C NMR spectra and FT-IR. The degree of quaternization of the pyridine groups on the side chain was about 34% as determined from UV−vis titration (see Supporting Information).

Methods. *Light Scattering.* Light scattering at an angle of 90° was performed with an ALV light scattering apparatus, equipped with a 400 mW argon ion laser operating at a wavelength of 532 nm. All the measurements were performed at room temperature. The light scattering intensity is expressed as the excess Rayleigh ratio R_θ divided by the polymer concentration. R_θ is obtained as

$$R_\theta = \frac{I_{sample} - I_{solvent}}{I_{toluene}} \times R_{toluene} \times \frac{n^2_{solvent}}{n^2_{toluene}} \quad (1)$$

where I_{sample} is the scattering intensity of the micellar solution and $I_{solvent}$ is the intensity of the solvent. $I_{toluene}$ is the scattering intensity of toluene (the reference), and $R_{toluene}$ is the known Rayleigh ratio of toluene (2.1×10^{-2} m^{-1}).

The Rayleigh ratio can be linked to the concentration and mass of the scattering objects:

$$\frac{K_R C}{R_\theta} = \frac{1}{M} \times \frac{1}{P(qR)} \times \frac{1}{S(q)} \quad (2)$$

where $C_{particle}$ is the weight concentration of micelles, $M_{particle}$ is their molar mass, and q is the scattering vector. $P(q)$ and $S(q)$ are the form factor and the structure factor, respectively. K is the optical constant defined as

$$K = \frac{4\pi^2 n^2}{N_{Av}\lambda_0^4}\left(\frac{dn}{dc}\right)^2 \quad (3)$$

where n is the refractive index of solvent, N_{Av} is Avogadro's number, λ_0 is the wavelength of the incoming beam (532.0 nm), and dn/dc is the refractive index increment of the Zn-L-P4VP$_{48}$-*b*-PEO$_{193}$ micelles. We measured dn/dc of the micellar solutions using a differential refractive index detector (Shodex RI-71).

In our experiments, the scattering vector $q = (4\pi n/\lambda_0)\sin(\theta/2)$ is ~0.023 nm^{-1} (θ = 90°), so that qR is small for the micelles (which have a radius on the order of 15 nm). We therefore assume that $P(qR) = 1$. At low concentrations, the structure factor can be approximated as

$$\frac{1}{S(q)} = 1 + 2B_2\frac{C}{M} \quad (4)$$

Substitution into eq 2, we get

$$\frac{K_R C}{R_\theta} = \frac{1}{M} + 2B_2\frac{C}{M^2} \quad (5)$$

By plotting K_RC/R_θ versus C, we can obtain the molar mass of the micelles from the intercept, from which we can obtain the aggregation number of the micelles. The second virial coefficient B_2 obtained from the slope of the curve is used to calculate the effective excluded volume (V_{eff}) and radius (R_{eff}): $B_2 = {}^1/_2 N_{Av} V_{eff}$, $V_{eff} = {}^4/_3 \pi R_{eff}^3$.

The hydrodynamic radius of the micelles was measured with dynamic light scattering. Intensity correlation functions were measured using an ALV-7002 digital correlator and converted to the field autocorrelation function $g_1(\tau)$. For a system consisting of polydisperse particles, this field correlation function can be written as an integral sum of decay curves:

$$g_1(\tau) = \int_\infty^0 G(\Gamma)e^{-\Gamma\tau}\,d\Gamma \quad (6)$$

where $G(\Gamma)$ is an intensity-weighted coefficient. First, we used the cumulant expansion method[27] to obtain the average decay rate $\langle\Gamma\rangle$, from which we calculate the mean apparent hydrodynamic radius (R_h)

$$R_h = kTq^2/6\pi\eta\langle\Gamma\rangle \quad (7)$$

where k is the Boltzmann constant, T is the absolute temperature, and η is the viscosity of the solvent. Second, regularized Laplace inversion of eq 6 using the CONTIN method[28,29] was used to find the intensity-weighted distribution of decay rates, which we convert into an intensity-weighted size distribution using eq 7.

Cryogenic Transmission Electronic Microscopy (Cryo-TEM). A few microliters of sample were placed on a Quantifoil 3.5/1 holey carbon-coated grid, and the excess of liquid was removed with filter paper, followed by shooting the grid into liquid ethane cooled to −170 °C. The sample vitrification procedure was carried out using Vitrobot (FEI, Eindhoven, The Netherlands) equipped with humidity and temperature chamber. Samples were studied in a Philips CM12 cryo-electron microscope operating at 120 kV with a Gatan model 626 cryo-stage. Images were recorded under low-dose conditions with a slow-scan CCD camera (Gatan, model 794). For each sample, images were collected for a number of different regions in the sample.

RESULTS AND DISCUSSION

The terdendate ligand group chosen in this work is chelidamic acid (also known as dipicolinic acid), a widely studied chelate group for building coordination structures.[30] NMR and FT-IR spectra confirm that the ligand groups are attached on the PVP

block successfully. The degree of quaternization of pyridine groups is determined by a UV−vis titration with Fe^{3+} and was found to be around 34% (see Supporting Information).

As shown in Scheme 1, the modified copolymer L-P4VP$_{48}$-*b*-PEO$_{193}$ has both positive charge on the quaternized pyridinium group and negative charges on the carboxylic groups. Hence, we first studied the self-assembly of this diblock copolymer as a function of pH in the absence of metal ions. The L-P4VP$_{48}$-*b*-PEO$_{193}$ becomes soluble in water above pH 6 (Figure 1a), where most of the carboxylic groups dissociate and the net charge of the polymer is negative. Decreasing the pH below 6 leads to the partial protonation of the carboxylic groups and a decrease of the overall net charge of the polymer. We find that the diblock copolymers start to aggregate below pH 6, initially forming nanoparticles with a hydrodynamic radius around 90 nm. These particles are not stable and a precipitate is formed after a few hours. However, the white precipitation can be dissolved completely by adding salt (Figure 1b). This strongly suggests that the aggregates are formed by electrostatic interaction between the positive charges on the pyridinium group and the negative charges of the carboxylic group. The pH-dependent aggregation behavior of L-P4VP$_{48}$-*b*-PEO$_{193}$ is completely different from that of unmodified P4VP$_{48}$-*b*-PEO$_{193}$ copolymer. The latter is soluble in water at low pH (<5) and forms micelles above pH 5 (Supporting Information), based on hydrophobic interaction between the PVP blocks.[31] The light scattering intensity in Figure 1a shows a maximum around pH 4, which is likely to be the isoelectric point of L-P4VP$_{48}$-*b*-PEO$_{193}$. Below pH 4, also the second carboxylic group of the ligand becomes protonated and the polymer acquires an overall positive charge, leading to the redissolution of the polymer.

Scheme 1. Structure of L-P4VP$_{48}$-*b*-PEO$_{193}$ Polymers (top) and Illustration of the Formation of Zn-L-P4VP$_{48}$-*b*-PEO$_{193}$ Micelles (bottom)[a]

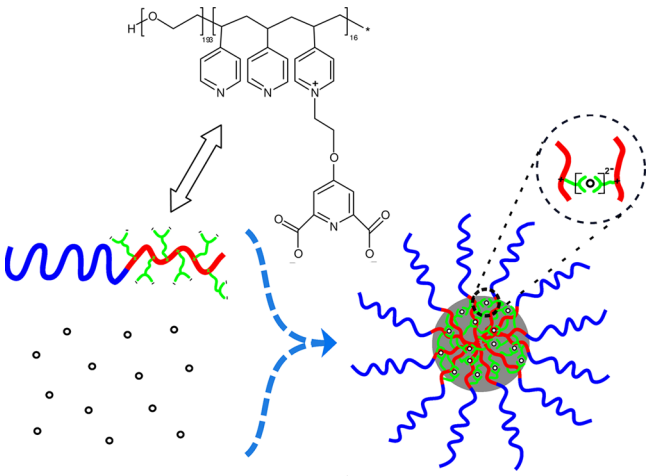

[a]Small dots represent the Zn^{2+} ions.

To study micelle formation with metal ions (Zn^{2+}, added in the form of a $Zn(NO_3)_2$ solution), we choose conditions (pH 6, 0.1 M NaCl) where the L-P4VP$_{48}$-*b*-PEO$_{193}$ polymer dissolves completely, so that any aggregate formation can be ascribed to the action of the metal ions. Indeed, the scattering intensity of the L-P4VP$_{48}$-*b*-PEO$_{193}$ solution in the absence of metal salt is very low, but it increases strongly when Zn^{2+} is added to the solution. Figure 2a shows the light scattering intensity and hydrodynamic radius of Zn-L-P4VP$_{48}$-*b*-PEO$_{193}$ micelles formed at different metal ion to ligand ratios M/L as a function of time. While the size of the scattering objects remains more or less constant in time, the intensity first increases rapidly, followed by a more gradual increase over several days. To explain this, we hypothesize that, upon adding Zn^{2+} to the block copolymer solution, we do not only obtain micellar aggregates but also smaller intramolecular complexes, where one Zn^{2+} ion binds with two ligands from the same polymer chain. The latter do not contribute much to the scattering intensity compared to the micelles. Our observation that the intensity keeps increasing slowly after the initial rapid increase must then imply that some of the intramolecular complexes convert into intermolecular complexes to form more micelles. Apparently, there is an energy barrier associated with this reorganization, which makes further aggregation a slow process, leading to a slow increase of the intensity. This two-step scenario must imply that intermolecular complexes are more favorable than intramolecular complexes. Probably, the polymer chain must bend or twist slightly in order to form an intramolecular complex, leading to a strained or low-entropy conformation. This strain is released when intermolecular complexes are formed. To test this two-step hypothesis, we measured the increase of light scattering intensity of Zn-L-P4VP$_{48}$-*b*-PEO$_{193}$ micelles at different polymer concentrations with M/L fixed at 0.5. Both the probabilities of inter- and intramolecular complex formation and the rate of reorganization should depend on the polymer concentration, so we expect a faster micelle formation at higher polymer concentration. As shown in Figure 2b, the intensity of micelles at higher polymer concentration indeed shows a faster increase than that of

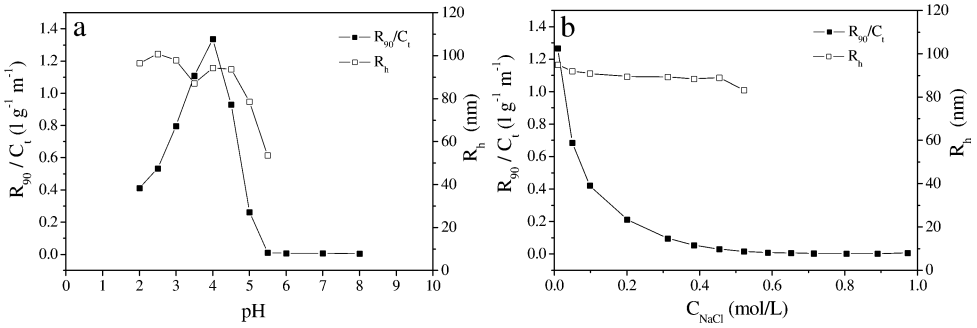

Figure 1. (a) Light scattering intensity (expressed by the excess Rayleigh ratio R_{90} divided by the total polymer concentration) and hydrodynamic radius of aggregates from L-P4VP$_{48}$-*b*-PEO$_{193}$ polymers in the absence of metal salt at different pH (0.64 g/L polymer). (b) The effect of salt on the intensity and size of aggregates from P4VP$_{48}$-*b*-PEO$_{193}$ formed at pH 4.

dx.doi.org/10.1021/ma301323z | *Macromolecules* 2012, 45, 7179−7185

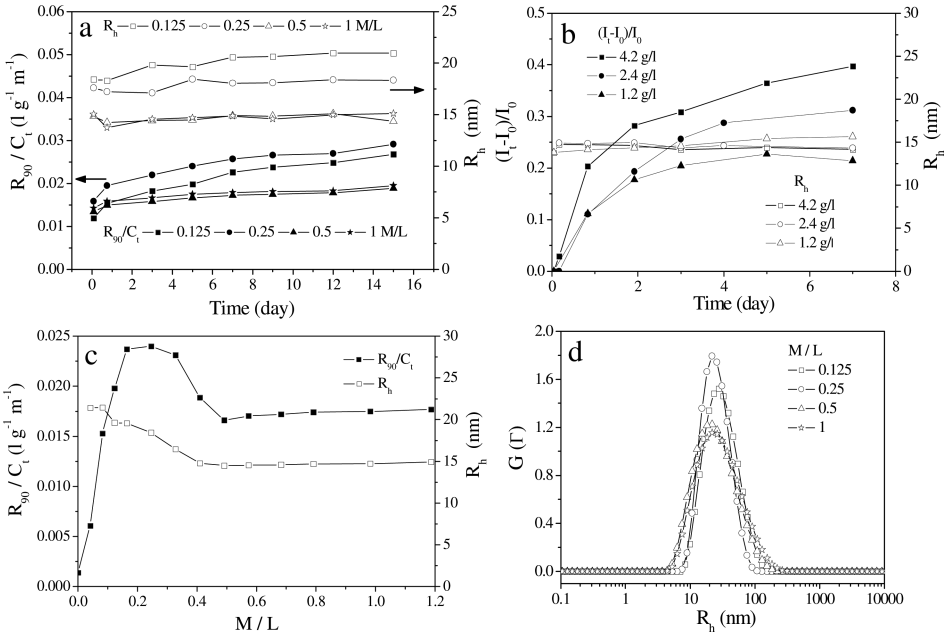

Figure 2. (a, b) Variations of light scattering intensity and hydrodynamic radius of Zn-L-P4VP$_{48}$-*b*-PEO$_{193}$ micelles formed at different M/L ratios (a) and different polymer concentrations (b). (c) Light scattering intensity and hydrodynamic radius as a function of the M/L ratio. (d) CONTIN analysis of particle size and intensity-weighted size distribution of Zn-L-P4VP$_{48}$-*b*-PEO$_{193}$ micelles formed at different M/L ratios (measured after 5 days). For (a, c, d), polymer concentration is fixed at 1.2 g/L.

micelles at lower polymer concentration, while the micelle size at all polymer concentrations hardly changes over time.

Figure 2c shows the light scattering intensity and hydrodynamic radius of Zn-L-P4VP$_{48}$-*b*-PEO$_{193}$ micelles as a function of the ratio between metal ion and ligand group concentration, M/L. All data points in this figure correspond to the light scattering intensity after an equilibration time of 5 days after mixing the components directly at the desired ratio. Surprisingly, the intensity varies nonmonotonically with M/L ratio. Around M/L equal to 0.3, the intensity goes through a maximum and then decreases until it reaches a constant value around M/L 0.5, where every Zn^{2+} ion can coordinate two ligand groups. Adding more metal ions (up to a ratio M/L of 1.2) does not lead to a decrease in intensity, indicating that an excess of Zn^{2+} ions does not disrupt the formed micelles. The hydrodynamic radius decreases monotonically from 21 nm at M/L 0.1 to 15 nm at M/L 0.5 and then becomes constant for M/L > 0.5. However, additional experiments indicate that the micellar objects are not equilibrium structures, even after several days. Adding additional Zn^{2+} to a 1 day old micelle solution prepared at M/L 0.25 did not lead to a decrease in size. Likewise, adding additional polymer to a solution prepared initially at M/L 0.5 did not give the same size as for a solution which is prepared directly at M/L 0.25. This means that the coordination interaction is quite strong in this system, and the formed micelles are nonequilibrium structures. The CONTIN results (Figure 2d) confirm the micellar size and indicate that there is one dominant kind of particle in solution at all M/L ratios. We also characterized the micelles with cryo-TEM. As shown in Figure 3, at M/L = 0.25, we see objects with radii of 5−10 nm. We presume that these structures are the micellar cores, where the metal ions reside. The corona of the PEO blocks provides insufficient contrast to be visible. Comparing the size of the core to the hydrodynamic radius (20 nm at this ratio), we find that the corona has a thickness around 10 nm, in agreement with values found for other micelles.[16,32] At M/L

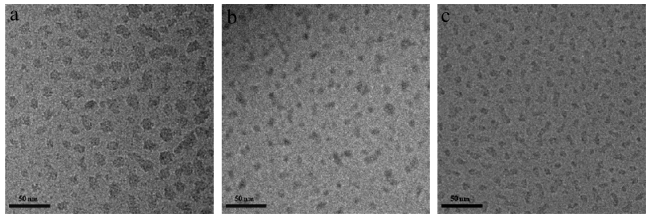

Figure 3. Cryo-TEM images of Zn-L-P4VP$_{48}$-*b*-PEO$_{193}$ micelles at different M/L: (a) 0.25, (b) 0.5, and (c) 1 (polymer concentration is fixed at 2.53 g/L, MES buffer, pH 6, 0.1 M NaCl, measured after 5 days).

ratios of 0.5 and 1 the micellar core is smaller, around 3−6 nm. Hence, the decrease in light scattering intensity and hydrodynamic radius seems to be caused by a decrease in size of the core.

What causes this decrease in core size upon increasing the metal concentration? One possible explanation is the repulsion between the unoccupied ligands. When a Zn^{2+} ion binds to two ligand groups, the overall charge of the L-Zn-L complex is −2, which just compensates the two positive charges of the pyridine groups to which the ligands are attached (see Scheme 1). This means that at a M/L ratio of 0.5, where all the ligand groups are involved in a L-M-L complex, the overall charge of the polymer approaches zero. The attraction between the negative L-M-L complexes and the positive pyridine groups may then lead to a compaction of the micellar core. At M/L ratios below 0.5, there are still unoccupied ligand groups on the polymer chain. The repulsion between them then probably prevents compaction of the core, resulting in the larger sizes seen with cryo-TEM and light scattering. We tried to measure zeta potentials of the Zn-L-P4VP$_{48}$-*b*-PEO$_{193}$ micelles in the solution, but unfortunately we could not obtain reliable data due to the electrostatic screening of the background electrolyte (0.1 M NaCl). Note that the electrostatic screening length does not vary

dx.doi.org/10.1021/ma301323z | *Macromolecules* 2012, 45, 7179−7185

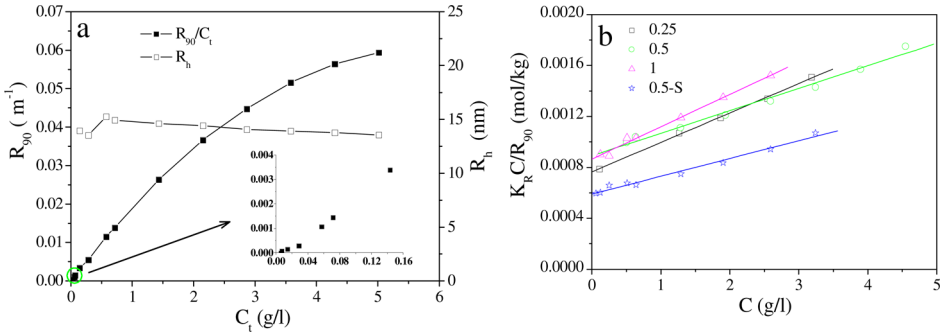

Figure 4. (a) Light scattering intensity and hydrodynamic radius versus total concentration of polymer and Zn^{2+}. Inset shows a zoom-in for low concentrations. (b) K_RC/R_{90} is plotted as a function of C ($C = C_t$ − CMC, C_t is the total concentration of polymer and Zn^{2+}). Zn-L-P4VP$_{48}$-*b*-PEO$_{193}$ micelles are prepared at M/L 0.25, 0.5, and 1 in 20 mM MES buffer, pH 6, 0.1 M NaCl; the 0.5-S sample is prepared at M/L 0.5, in 20 mM MES buffer, pH 6, 0.8 M NaCl.

significantly in our experiments because the salt concentration changes by at most a few percent upon adding metal due to the relatively high concentration of background electrolyte.

An alternative explanation for the decrease in size upon increasing the M/L ratio is a decrease in aggregation number of the micelles going from from low to high M/L. We carry out light scattering experiments at different concentrations to test this. Figure 4a shows the changes of light scattering intensity and hydrodynamic radius of Zn-L-P4VP$_{48}$-*b*-PEO$_{193}$ micelles upon diluting with buffer solution. By extrapolating the intensity to the baseline, we found that the critical micelle concentration (CMC) is about 0.02 g/L. The aggregation number of micelles formed at different M/L ratios is obtained by plotting K_RC/R_{90} as a function of the concentration C (Figure 4b) and using eq 5. The results are summarized in Table 1. Indeed, the aggregation number of the micelles is larger at M/L < 0.5 than at M/L ≥ 0.5, while the CMC does not depend strongly on the M/L ratio. The second virial coefficient B_2 has a minimum at M/L 0.5, where the micelles are most compact.

Table 1. Critical Micelle Concentration (CMC), Aggregation Number (N_{agg}), Second Virial Coefficient B_2, and Effective Excluded Volume V_{eff} and Corresponding Radius R_{eff} of the Micelles as a Function of the M/L Ratio and the Salt Concentration[a]

M/L	CMC (g/L)	d*n*/d*c* (m^3/kg)	N_{agg}	B_2 (m^3/mol)	V_{eff} (m^3)	R_{eff} (nm)
0.25	0.019	1.34×10^{-4}	71	198	6.58×10^{-22}	54
0.5	0.020	1.25×10^{-4}	60	111	3.68×10^{-22}	44
1	0.010	1.25×10^{-4}	62	171	5.68×10^{-22}	51
0.5-S	0.010	1.25×10^{-4}	91	202	6.70×10^{-22}	54

[a]Values were obtained by analyzing the light scattering data shown in Figure 4.

At first sight, it seems surprising that the aggregation number is larger at low M/L ratios, where the electrostatic repulsion between the unoccupied ligand groups is stronger. However, it must be kept in mind that the micelles are not equilibrium structures, so that the aggregation number is determined largely by kinetic effects. Probably, at M/L < 0.5 the metal ions have more opportunities to cross-link a larger number of polymer chains, leading to larger aggregation numbers at smaller M/L ratios.

As mentioned in the Introduction, Zn-L-P4VP$_{48}$-*b*-PEO$_{193}$ micelles are formed based on the strong coordination between ligand and metal ions. One of the advantages of using coordination bonds as the direct driving force for micellization is that coordination bonds are not very sensitive to added salt. To test whether this reduced sensitivity indeed leads to more stable micelles, we investigated the effect of the salt concentration on the Zn-L-P4VP$_{48}$-*b*-PEO$_{193}$ micelles (M/L 0.5). Figure 5a shows that the light scattering intensity and hydrodynamic radius of Zn-L-P4VP$_{48}$-*b*-PEO$_{193}$ micelles do not change up to salt concentration as high as 0.4 M NaCl and then even go up as the salt concentration increases further to 1 M. The increase in intensity at high salt concentration can be explained by the screening effect of the salt ions that weakens the electrostatic interaction between the positively charged pyridine groups and the negatively charged metal complexes, leading to swelling of the core (without disrupting it). This also leads to an increase of the aggregation number of the micelles, and an increase of the excluded volume, as shown by the light scattering results (Table 1). Our results contrast strongly with previous observations for metal-containing complex coacervate core micelles based on electrostatic coassembly, where the scattering intensity decreased strongly upon adding salt,[17,18] and confirm that the micelles do not dissociate at high ionic strength. The high stability of the micelles is due to the strong coordination bonds between the chelidamic acid ligand groups and Zn^{2+} ions. To test how strong these bonds are, we added EDTA to the micellar solution as a competing ligand. We did not notice any change in the light scattering intensity and hydrodynamic radius of the micellar solution after adding EDTA over a period of 8 days, indicating that the coordination bonds that keep the micelles together are indeed very strong. Probably, the cross-linked micellar structure and the favorable electrostatic interaction with the pyridinium groups make the coordination bonds even stronger than for free chelidamic acid.

■ CONCLUSION

We report a stable metal-containing polymer micelle system. A diblock copolymer P4VP$_{48}$-*b*-PEO$_{193}$ is modified with a terdendate ligand grafted to the PVP block. Upon mixing with metal ions, micelles are formed, directly driven by the metal−ligand coordination interaction. The formed Zn-L-P4VP$_{48}$-*b*-PEO$_{193}$ micelles have a hydrodynamic radius of about 15 nm, while the radius of the micellar core is around 5 nm. Adding salt and EDTA hardly affects the Zn-L-P4VP$_{48}$-*b*-PEO$_{193}$ micelles, confirming the high stability of the structures. Preliminary results show that micelles can also be made with other metal ions than Zn^{2+} (Ni^{2+}, Mn^{2+}, Gd^{3+}), demonstrating

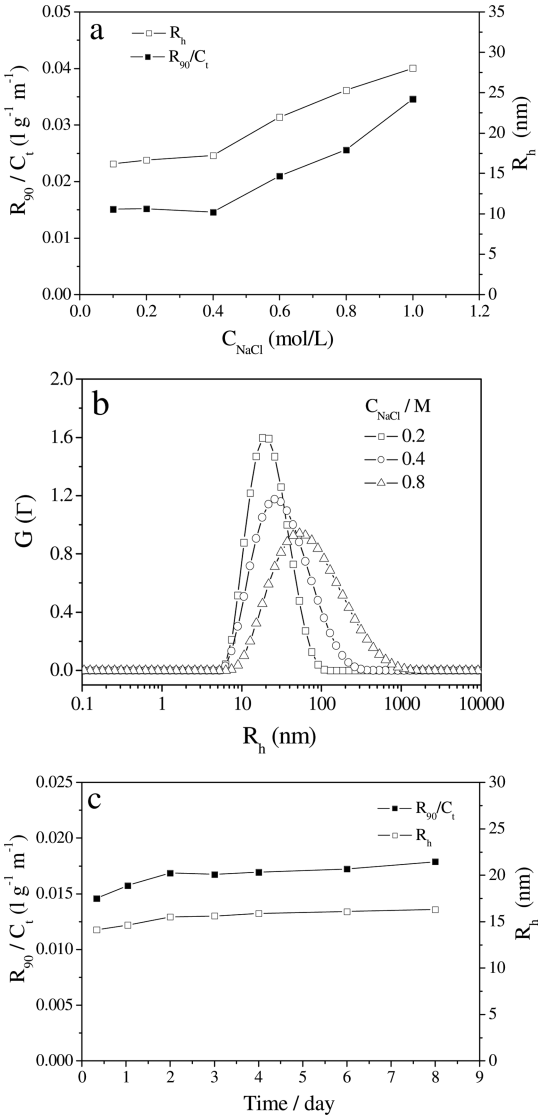

Figure 5. (a) Effect of salt on the scattering intensity and hydrodynamic radius of Zn-L-P4VP$_{48}$-*b*-PEO$_{193}$ micelles. (b) CONTIN analysis of particle size and size distribution at different salt concentration. (c) Variations of intensity and radius of micelles with EDTA in solution (same amount with chelidamic acid groups).

the general applicability of this strategy for making stable metal-containing micelles.

■ ASSOCIATED CONTENT

Ⓢ Supporting Information

^{1}H NMR and ^{13}C NMR spectra of the synthesized polymer; FT-IR spectra and UV−vis titration curve of the synthesized polymer; light scattering data of unmodified P4VP$_{48}$-*b*-PEO$_{193}$ polymer. This material is available free of charge via the Internet at http://pubs.acs.org.

■ AUTHOR INFORMATION

Corresponding Author

*E-mail: junyou.wang@wur.nl.

Notes

The authors declare no competing financial interest.

■ ACKNOWLEDGMENTS

The authors thank Henk van As and Pieter de Waard (Laboratory of Biophysics and Wageningen Nuclear Magnetic Resonance Center, Wageningen University, Dreijenlaan 3, 6703 HA Wageningen, The Netherlands) for help with NMR experiments and Remco Fokkink (Laboratory of Physical Chemistry and Colloid Science, Wageningen University, Dreijenplein 6, 6703 HB Wageningen, The Netherlands) for the help of light scattering data analysis.

■ REFERENCES

(1) Wang, X.; McHale, R. *Macromol. Rapid Commun.* **2010**, *31*, 331−350.
(2) Paz, F. A. A.; Klinowski, J.; Vilela, S. M. F.; Tome, J. P. C.; Cavaleiro, J. A. S.; Rocha, J. *Chem. Soc. Rev.* **2012**, *41*, 1088−1110.
(3) Winter, A.; Hager, M. D.; Newkome, G. R.; Schubert, U. S. *Adv. Mater.* **2011**, *23*, 5728−5748.
(4) Kurth, D. G.; Higuchi, M. *Soft Matter* **2006**, *2*, 915−927.
(5) Moughton, A. O.; O'Reilly, R. K. *Macromol. Rapid Commun.* **2010**, *31*, 37−52.
(6) Schubert, U. S.; Eschbaumer, C. *Angew. Chem., Int. Ed.* **2002**, *41*, 2892−2926.
(7) Kimpe, K.; Parac-Vogt, T. N.; Laurent, S.; Pierart, C.; Elst, L. V.; Muller, R. N.; Binnemans, K. *Eur. J. Inorg. Chem.* **2003**, 3021−3027.
(8) Gianolio, E.; Giovenzana, G. B.; Longo, D.; Longo, I.; Menegotto, I.; Aime, S. *Chem.—Eur. J.* **2007**, *13*, 5785−5797.
(9) Owen1, T.; Butler, A. *Coord. Chem. Rev.* **2011**, *255*, 678−687.
(10) Gohy, J. F.; Lohmeijer, B. G. G.; Schubert, U. S. *Macromolecules* **2002**, *35*, 4560−4563.
(11) Gohy, J. F.; Lohmeijer, B. G. G.; Schubert, U. S. *Macromol. Rapid Commun.* **2002**, *23*, 555−560.
(12) Ott, C.; Hoogenhoom, R.; Hoeppener, S.; Wouters, D.; Gohy, J. F.; Schubert, U. S. *Soft Matter* **2009**, *5*, 84−91.
(13) Zhou, G.; He, J.; Harruna, I. I. *J. Polym. Sci., Part A: Polym. Chem.* **2007**, *45*, 4204−4210.
(14) Moughton, A. O.; O'Reilly, R. K. *J. Am. Chem. Soc.* **2008**, *130*, 8714−8725.
(15) Joubert, M.; In, M. *ChemPhysChem* **2008**, *9*, 1010−1019.
(16) Yan, Y.; Besseling, N. A. M.; de Keizer, A.; Marcelis, A. T. M.; Drechsler, M.; Cohen Stuart, M. A. *Angew. Chem., Int. Ed.* **2007**, *46*, 1807−1809.
(17) (a) Yan, Y.; de Keizer, A.; Cohen Stuart, M. A.; Drechsler, M.; Besseling, N. A. M. *J. Phys. Chem. B* **2008**, *112*, 10908−10914.
(18) Wang, J. Y.; de Keizer, A.; Fokkink, R.; Yan, Y.; Cohen Stuart, M. A.; van der Gucht, J. *J. Phys. Chem. B* **2010**, *114*, 8313−8319.
(19) Bronich, T. K.; Keifer, P. A.; Shlyakhtenko, L. S.; Kavanov, A. V. *J. Am. Chem. Soc.* **2005**, *127*, 8236−8237.
(20) Bronstein, L. M.; Sidorov, S. N.; Zhirov, V.; Zhirov, D.; Kabachii, Y. A.; Kochev, S. Y.; Valetsky, P. M.; Stein, B.; Kiseleva, O. I.; Polyakov, S. N.; Shtykova, E. V.; Nikulina, E. V.; Svergun, D. I.; Khokhlov, A. R. *J. Phys. Chem. B* **2005**, *109*, 18786−18798.
(21) Bronstein, L. M.; Sidorov, S. N.; Valetsky, P. M. *Langmuir* **1999**, *15*, 6256−6262.
(22) Nyman, C. J. *J. Am. Chem. Soc.* **1953**, *75*, 3575−3576.
(23) Bunting, J. W.; Thong, K. M. *Can. J. Chem.* **1970**, *48*, 1654−1656.
(24) Vermonden, T.; van der Gucht, J.; de Waard, P.; Marcelis, A. T. M.; Besseling, N. A. M.; Sudholter, E. J. R.; Fleer, G. J.; Cohen Stuart, M. A. *Macromolecules* **2003**, *36*, 7035−7044.
(25) Vermonden, T.; Branowska, D.; Marcelis, A. T. M.; Sudholter, E. J. R. *Tetrahedron* **2003**, *59*, 5039−5045.
(26) Froidevaux, P.; Harrowfield, J. M.; Sobolev, A. N. *Inorg. Chem.* **2000**, *39*, 4678−4687.
(27) Koppel, D. *J. Chem. Phys.* **1972**, *57*, 4814−4820.
(28) Provencher, S. W. *Comput. Phys. Commun.* **1982**, *27*, 213−227.
(29) Provencher, S. W. *Comput. Phys. Commun.* **1982**, *27*, 229−242.

(30) Yan, Y.; de Keizer, A.; Cohen Stuart, M. A.; Besseling, N. A. M. *Adv. Polym. Sci.* **2011**, *242*, 91−115.
(31) Ma, L.; Kang, H. L.; Liu, R. G.; Huang, Y. *Langmuir* **2010**, *26*, 18519−18525.
(32) Wang, J. Y.; de Keizer, A.; van Leeuwen, H. P.; Yan, Y.; Vergeldt, F.; van As, H.; Bomans, P. H. H.; Sommerdijk, N. A. J. M.; Cohen Stuart, M. A.; van der Gucht, J. *Langmuir* **2011**, *27*, 14776−14782.